Clinical Cancer Research

Interleukin-27 Acts as Multifunctional Antitumor Agent in Multiple Myeloma

Claudia Cocco, Nicola Giuliani, Emma Di Carlo, et al.

Clin Cancer Res 2010;16:4188-4197. Published OnlineFirst June 29, 2010.

Published OnlineFirst June 29, 2010; DOI:10.1158/1078-0432.CCR-10-0173

Cancer Therapy: Preclinical

Clinical Cancer Research

Interleukin-27 Acts as Multifunctional Antitumor Agent in Multiple Myeloma

Claudia Cocco[1], Nicola Giuliani[3], Emma Di Carlo[4], Emanuela Ognio[2], Paola Storti[3], Manuela Abeltino[3], Carlo Sorrentino[4], Maurilio Ponzoni[5], Domenico Ribatti[6], and Irma Airoldi[1]

Abstract

Purpose: Multiple myeloma (MM) derives from plasmablast/plasma cells that accumulate in the bone marrow. Different microenvironmental factors may promote metastatic dissemination especially to the skeleton, causing bone destruction. The balance between osteoclast and osteoblast activity represents a critical issue in bone remodeling. Thus, we investigated whether interluekin-27 (IL-27) may function as an antitumor agent by acting directly on MM cells and/or on osteoclasts/osteoblasts.

Experimental Design: The IL-27 direct antitumor activity on MM cells was investigated in terms of angiogenesis, proliferation, apoptosis, and chemotaxis. The IL-27 activity on osteoclast/osteoblast differentiation and function was also tested. *In vivo* studies were done using severe combined immunodeficient/nonobese diabetic mice injected with MM cell lines. Tumors from IL-27– and PBS-treated mice were analyzed by immunohistochemistry and PCR array.

Results: We showed that IL-27 (*a*) strongly inhibited tumor growth of primary MM cells and MM cell lines through inhibition of angiogenesis, (*b*) inhibited osteoclast differentiation and activity and induced osteoblast proliferation, and (*c*) damped *in vivo* tumorigenicity of human MM cell lines through inhibition of angiogenesis.

Conclusions: These findings show that IL-27 may represent a novel therapeutic agent capable of inhibiting directly MM cell growth as well as osteoclast differentiation and activity. *Clin Cancer Res; 16(16); 4188–97. ©2010 AACR.*

Interleukin (IL)-27 is a heterodimeric cytokine belonging to the IL-12 family (1). It is composed of the EBV-induced 3 (EBI3) and p28 subunits that are homologues to the p40 and p35 chains of IL-12, respectively (2). IL-27 is produced by antigen-presenting cells, which protect their local microenvironment from host pathogens, and functions on different cell types expressing the full receptor (R) complex (3–7). The IL-27R contains the unique receptor subunit WSX-1 also known as IL-27Ra/TCCR, paired with the gp130 chain. Both chains are necessary for IL-27 signaling (8, 9). IL-27 is considered a proinflammatory and an anti-inflammatory cytokine (10, 11) that can inhibit TH1 (12–14), TH17 (15, 16), and TH2 responses (17, 18), and suppress the development of inducible regulatory T cells (19). IL-27, similarly to IL-12, shows antitumor activity in different tumors through indirect mechanisms such as induction of natural killer and CTL response or inhibition of angiogenesis primarily due to induction of CXCL10 and CXCL9 (20–26). Recently, it has been shown that IL-27 inhibits directly the proliferation of human melanoma cell lines expressing functional IL-27R (27), but there is no information on the role of IL-27 in human hematologic malignancies.

Multiple myeloma (MM) is a monoclonal postgerminal center tumor that has phenotypic features of plasmablasts/long-lived plasmacells and usually localizes at multiple sites in the bone marrow (BM; refs. 28). Pathogenesis of MM is complex and dependent on the interactions between tumor cells and microenvironment in the BM, the primary site of MM development (28, 29). Different cytokines, chemokines, and proangiogenic factors released in the tumor microenvironment are known to promote MM cell growth and metastatic dissemination, especially to the skeleton (29–31). MM represents the second most common hematologic malignancy worldwide, and its prognosis remains grim in

Authors' Affiliations: [1]Associazione Italiana per la Ricerca sul Cancro Laboratory of Immunology and Tumors, Department of Experimental and Laboratory Medicine, G. Gaslini Institute and [2]Animal Model Facility, Istituto Nazionale per la Ricerca sul Cancro, Genova, Italy; [3]Hematology and BMT Center, Department of Internal Medicine and Biomedical Science, University of Parma, Parma, Italy; [4]Department of Oncology and Neurosciences, "G. d'Annunzio" University and Ce.S.I. Aging Research Center, "G. d'Annunzio" University Foundation, Chieti, Italy; [5]Pathology Unit, Myeloma Unit, San Raffaele Scientific Institute, Milan, Italy; and [6]Department of Human Anatomy and Histology, University of Bari, Bari, Italy

Corresponding Author: Irma Airoldi, Associazione Italiana per la Ricerca sul Cancro Laboratory of Immunology and Tumors, Department of Experimental and Laboratory Medicine, G. Gaslini Institute, Genova, Italy. Phone: 39-0105636342; Fax: 39-0103779820; E-mail: irmaairoldi@ospedale-gaslini.ge.it.

doi: 10.1158/1078-0432.CCR-10-0173

Published OnlineFirst June 29, 2010; DOI:10.1158/1078-0432.CCR-10-0173

Translational Relevance

Multiple myeloma (MM) represents the second most common hematologic malignancy worldwide, and its prognosis remains grim in spite of advanced therapeutic approaches. Here, we show that human interluekin-27 (IL-27) directly inhibited MM cell growth both *in vitro* and *in vivo* primarily through the inhibition of angiogenesis. IL-27 also damped the differentiation and activity of osteoclasts, and stimulated osteoblast proliferation. Our results open new perspectives for MM therapy because IL-27 may block MM progression and metastatic bone resorption.

spite of advanced therapeutic approaches (32). Thus, novel therapeutic strategies are warranted to improve MM prognosis. With this background, we have asked whether IL-27 may function as antitumor agent against human MM.

Materials and Methods

Patients

The study design was approved by the Ethical Committee of the University of Parma, Parma, Italy. Twelve MM patients were studied. Of them, five were male and seven were female. Patient age ranged from 49 to 92 years. Nine patients had stage IIIa, two had stage IIIb, and one had stage Ia disease, according to the Durie and Salmon staging system (33). The monoclonal serum component was IgGκ in seven cases, IgGλ in four cases, and IgAκ in one case. BM infiltration with malignant plasma cells at diagnosis ranged from 30% to 75%. At study, all patients were nontreated. Aliquots of BM aspirates done for clinical evaluation were obtained after informed consent at diagnosis in 10 cases and at relapse in the remaining two.

Cell culture, antibodies, reagents, and flow cytometry

The human U266, Karpas 620, RPMI 8226, H-Sultan, OPM-2, JJN3, XG-1, XG-6, and NCI-H929 MM cell lines (American Type Culture Collection cell bank) were cultured in RPMI 1640 with 10% FCS (Seromed-BiochromKG). Human recombinant (hr) IL-27 (R&D System) was used at different concentrations following titration experiments (50-100 ng/mL in most cases). Fluorochrome-conjugated CD19, CD20, CD38, CD138, anti-human IL6, anti-human IFN-γ, and anti-human immunoglobulin were from BD Pharmingen. Anti-Ki67 was from DAKO, Dakocytomation, Glostrup, DK. Anti-human WSX-1 monoclonal antibody (mAb) was from R&D System. Isotype-matched antibodies of irrelevant specificity (Caltag) were used as controls. Cells were scored using a FACSCalibur analyzer (BD Biosciences), and data were processed using CellQuest software (BD).

Cell proliferation and apoptosis assays

The human NCI-H929, U266 MM cell lines and the osteoblastic Hobit cells (kindly gift by Dr. Riggs, Mayo Clinic, Rochester, MN; ref. 34) were cultured for 5, 16, 24, 48, and 72 hours with or without 100 ng/mL hrIL-27. MM cells were then stained with Ki67 mAb and analyzed by flow cytometry. Apoptosis was assessed using AnnexinV/FITC kit (Bender MedSystems). Hobit cell proliferation was evaluated by MTT Cell proliferation assay (Cayman Chemical). In some experiments, BM stromal cells (SC), obtained from BM mononuclear cells of MM patients as previously described (35), were cultured 48 hours in the presence or absence of MM cells from patients (n = 2; BMSC/MM ratio, 1:5) with or without IL-27 (50 ng/mL). Cells were than tested for apoptosis by flow cytometry

ELISA

Culture supernatants, collected 48 hours after IL-27 treatment, were tested in triplicate using the human 10 cytokine Bio-Plex Assay (IL-12, IFN-γ, IL-10, IL-6, IL-8, IL-4, IL-5, IL-1β, and tumor necrosis factor α and β; Bio-Rad Laboratories, Inc.).

Mice studies

Four- to six-week-old severe combined immunodeficient-nonobese diabetic (SCID-NOD) mice (Harlan Laboratories) were housed under specific pathogen-free conditions. All procedures were done in the respect of the National and International current regulations (D.l.vo 27/01/1992, n.116, European Economic Community Council Directive 86/609, OJL 358, Dec. 1, 1987).

Two groups of 16 animals each were injected i.p. with 8×10^6 NCI-H929 cells. Two additional groups of 10 mice each were injected s.c. with 8×10^6 U266 cells. One group of mice for each combination was treated with three weekly doses of hrIL-27 (1 μg/mouse/dose) starting from 8 hours after tumor cells injection. The other group of mice from each combination was injected with PBS (controls) according to the same time schedule. Twenty-one days after tumor cell inoculation, mice were sacrificed and tumor mass was measured, as previously described (23).

Chorioallantoic membrane assay

Chorioallantoic membrane (CAM) assay was done as reported (36) and was loaded with 1 μL of PBS (negative control), 1 μL of PBS with 250 ng vascular endothelial growth factor (VEGF; R&D Systems) as positive control, 1 μL of medium from NCI-H929 cells or purified MM cells from patients cultured 48 hours with or without 100 ng/mL hrIL27, and 1 μL of medium containing hrIL-27 (100 ng/mL). All supernatants were tested in triplicate, and means ± SD were calculated. CAM were examined daily until day 12 and photographed *in ovo* with a stereomicroscope equipped with a camera and image analyzer system (Olympus Italia). On day 12, the angiogenic response was evaluated by the image analyzer system as the number of vessels converging toward the sponges.

Published OnlineFirst June 29, 2010; DOI:10.1158/1078-0432.CCR-10-0173

Osteoclastogenesis and osteoclast activity

Osteoclast were generated from peripheral blood (PB) $CD14^+$ monocytes of MM patients ($n = 3$) or of healthy donors ($n = 3$). Cells were isolated by immunomagnetic beads (Miltenyi Biotec). Monocytes were cultured 28 days in α-MEM with 10% fetal bovine serum (Invitrogen) and then plated in eight-well slides (Nalgene Nunc A/S Roskilde) at the density of $7.5 \times 10^5/cm^2$ with RANKL (Pierce; 50 ng/mL) and M-CSF (Pierce; 25 ng/mL).

Osteoclast phenotype was assessed after 28 days by cytochemical analysis of tartrate-resistant acid phosphatase (TRAP) using a commercial kit (Sigma Aldrich). HrIL-27 was added (100 ng/mL) to the above monocyte cultures at day 3, 7, 14, and 21. $TRAP^+$ multinucleated cells containing more than five nuclei (mature osteoclast) were counted by optical microscopy. Each sample was cultured in duplicate, and 40 microscopy fields at high magnification (×400) were evaluated for each well. The results were expressed as mean number of osteoclast counted per well ± SD.

Pit assay was done to evaluate the osteoclast activity. To this end, osteoclast generated as above and cultured 28 days with or without hrIL-27 were tested using bone slices (Pantec s.r.l.), and pits were counted by microscopy. Images were obtained on a Nikon Eclipse TE 300 microscope at 10X/0.13 using a DS-U1 digital slight and at 4×/0.12 objective lens.

Osteoblast marker evaluation and bone nodule formation

Confluent osteoblastic cells Hobit were incubated in D-MEM and 10% fetal bovine serum with or without hrIL-27 (range, 50-100 ng/mL) for 48 hours. Cell lysates were prepared for Western blot analysis (37) to check collagen and osteocalcin expression. Polyclonal anti-Collagen I and osteocalcin antibody were from Santa Cruz Biotechnology. In other experiments, confluent Hobit cells were cultured with ascorbic acid (50 μg/mL) and Dexametasone (Sigma Aldrich; 1×10^{-8} mol/L), with β-glycerophosphate (Sigma Aldrich; 10 mmol/L) with or without hrIL-27 (50-100 ng/mL) for 1 to 2 weeks. Cells were fixed with cold formalin at 4°C, washed thrice with PBS, and stained with Alkaline Phosphatase semiquantitative histochemical kit (Sigma Aldrich), or fixed with 1:1 mixture (vol/vol) of 37% formaldehyde and ethanol for 5 minutes, washed thrice with PBS, and stained for 10 minutes with a solution of 2% of Alizarid Red (Sigma Aldrich) at pH 4.2 for bone nodule evaluation.

PCR array

RNA was extracted from tumors removed from SCID-NOD mice or from $CD138^+$ MM cells cultured for 36 hours with or without (controls) hrIL-27 using Trizol from Invitrogen. Contaminant genomic DNA was removed by Dnase treatment (Qiagen GmbH). RNA was retrotranscribed by the RT^2 First Strand cDNA Synthesis kit (SABioscience).

Human Angiogenesis RT^2 PCR Array and RT^2 Real-Time SyBR Green/ROX PCR Mix were from SABioscience. PCR was done on the ABI Prism 7700 Sequence Detector (Applied Biosystems). Gene expression of IL-27–treated and control samples were analyzed separately in different PCRArray plates. For each plate, results were normalized on the median value of a set of housekeeping genes. Then, changes in gene expression between IL-27–treated and control samples were calculated using the ΔΔCt formula (38). Results from three different IL-27–treated and control samples were pooled and, according to the protocol, analyzed by the software provided by the manufacturer. A significant threshold of 4-fold change in gene expression corresponded to $P < 0.001$.

Histologic and immunohistochemical analyses

Tissue samples were formalin fixed, paraffin embedded, sectioned at 4-μm-thick sections, and stained with H&E. For immunohistochemistry, formalin-fixed, paraffin-embedded sections were immunostained with rabbit anti-human laminin (Biogenex), rabbit anti-human IL-6 (Abcam), or rabbit anti-human VEGF-C (Zymed), mouse anti-human Ki67 (DAKO), rabbit anti-mouse CD31 (Thermo Scientific), and rat anti-mouse F4/80 (Serotec) antibodies.

After washing, sections were overlaid with goat anti-rabbit immunoglobulin conjugated to peroxidase-labeled dextran (EnVision+Peroxidase, rabbit/mouse; Dakocytomation) for 30 minutes. Unbound immunoglobulin was removed by washing, and slides were incubated with avidin-biotin complex/alkaline phosphatase (DAKO) for 30 minutes, then sections were counterstained with H&E.

DNA fragmentation associated with apoptosis was detected in 4-μm tissue sections by terminal deoxynucleotidyl transferase–mediated dUTP nick end labeling staining with the ApopTag Plus Peroxidase *In situ* Apoptosis kit (Millipore) according to the manufacturer's protocol.

Statistical methods

Differences in the number of vessels formed in CAM assay and in Hobit cell proliferation cultured in the presence or absence of IL-27 were evaluated by Student's *t* test. Differences in tumor volume were calculated using Mann-Whitney test comparing two independent samples, with 99% confidence interval. All statistical tests were two tailed.

Results

IL-27R in human primary MM cells

First, we investigated the expression of the gp130 and WSX-1 chains of IL-27R in primary neoplastic cells isolated from the infiltrated BM of 12 MM patients. Figure 1A shows that WSX-1 expression was consistently detected in $CD138^+$ MM cells by flow cytometry. The gp130 chain was always detected in all samples (data not shown).

MM cells are known to release several proangiogenic factors (39); thus, we asked whether this feature was affected by IL-27. We incubated $CD138^+$ neoplastic cells from MM patients (patients #1, #2, #4, and #8) with hrIL-27 or medium for 48 hours and tested the angiogenic activity

Published OnlineFirst June 29, 2010; DOI:10.1158/1078-0432.CCR-10-0173

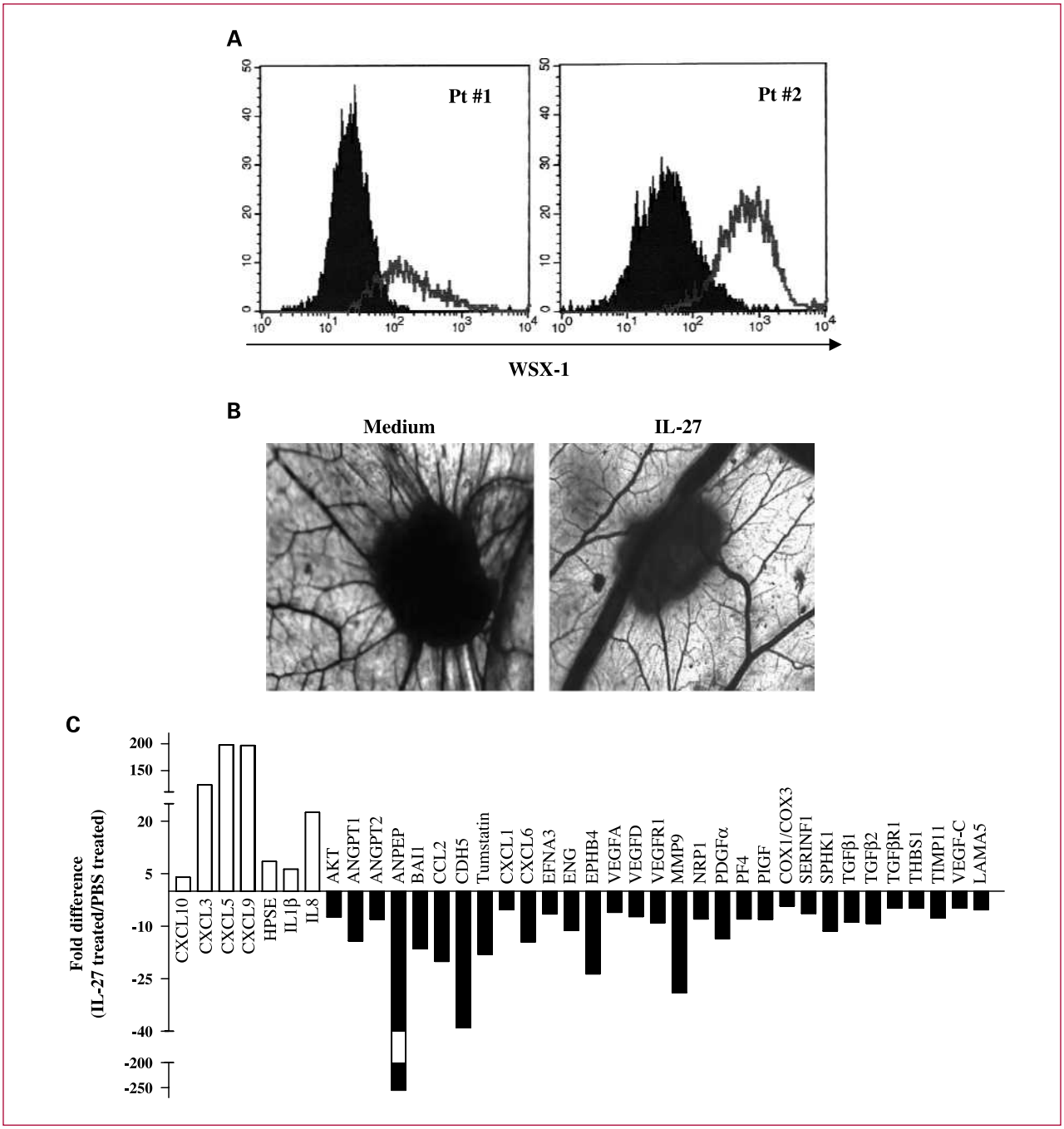

Fig. 1. A, WSX-1 surface expression in human CD138$^+$ primary MM cells. Open profile, WSX-1 staining; dark profile, isotype-matched mAb staining. B, angiogenic activity of supernatants from one representative (of four) CD138$^+$ MM sample cultured with or without IL-27. CAM-treated with sponges loaded with the conditioned medium from the nontreated cells were surrounded by allantoic vessels developing radially toward the implant in a spoked wheel pattern (left). When supernatant from the same MM sample cultured with hrIL27 was tested, a significant reduction of the angiogenic response was evident (right). Original magnification, ×50. C, CD138$^+$ primary MM cells were incubated with medium (n = 3) or hrIL-27 (n = 3) and tested for mRNA expression of 84 angiogenesis-related genes. Pooled results of three independent experiments are shown. Histogram represents fold differences of individual RNA expression between MM cells cultured with or without hrIL-27.

of culture supernatants by CAM assay. There were no significant differences in the proportions of viable cells (trypan blue staining) between cultures done with or without hrIL-27. CAM treated with sponges loaded with VEGF (positive control) or supernatants from primary MM cells were surrounded by allantoic vessels developing radially toward the implant in a "spoked wheel" pattern. In the representative experiment shown in Fig. 1B (left), the

Published OnlineFirst June 29, 2010; DOI:10.1158/1078-0432.CCR-10-0173

mean number of vessels formed by supernatant from MM cells (Pt #1) was 25 ± 4, whereas that formed by VEGF was 30 ± 5 (data not shown). No vascular reaction was detected around the sponges upon exposure to hrIL-27 diluted in medium at the same final concentration used to treat tumor cells (mean number of vessels, 7 ± 3 with or without IL-27). When the supernatants from hrIL-27–treated $CD138^+$ cells from the same MM patient was tested, a significant ($P < 0.001$) reduction of the angiogenic response was appreciable (mean number of vessels, 12 ± 3; Fig. 1B, right). Similar results with the same statistical significance were obtained when supernatants from the three remaining $CD138^+$ primary MM cell suspensions were tested (patient #2: mean number of vessels formed by nontreated supernatant was 22 ± 3 and 10 ± 2 by hrIL-27-treated supernatant. Patient #4: mean number of vessels formed by nontreated supernatant was 28 ± 4 and 12 ± 3 by hrIL-27–treated supernatant. Patient #8: mean number of vessels formed by nontreated supernatant was 25 ± 2 and 11 ± 2 by hrIL-27–treated supernatant).

Next, we investigated expression of proangiogenic and antiangiogenic genes in primary MM cells incubated with hrIL-27 or medium. Purified $CD138^+$ cells from three different MM patients (patients #1, #4, and #8) were cultured for 36 hours with or without hrIL-27.

Figure 1C shows the pooled results from the three samples analyzed by PCR array. HrIL-27 treatment significantly downregulated mRNA ($P < 0.001$) of a wide panel of proangiogenic genes including AKT, angiopoietin 1, angiopoietin 2, alanyl aminopeptidase, CCL2, laminin 5, matrix metalloproteinase 9, transforming growth factor β1 and β2, VEGF-A, VEGF-C, and VEGF-D, and upregulated mRNA of the antiangiogenic chemokines CXCL9 and CXCL10. Some proangiogenic genes including CXCL3 and CXCL5 were also upregulated in the same cells.

In experiments done in triplicate using three different primary MM cell suspensions, IL-27 did not attract tumor cells in chemotaxis assays nor affect proliferation, apoptosis, or cytokine release.

IL-27 inhibits osteoclast formation and stimulates osteoblast proliferation *in vitro*

The effect of IL-27 on osteoclast and osteoblast was next investigated. $CD14^+$ monocytes freshly isolated from PB of MM patients or healthy donors expressed WSX-1, by flow cytometry (Fig. 2A, left).

Three different osteoclast preparations were generated from PB $CD14^+$ monocytes of MM patients or normal donors. Cells were stained for TRAP to identify osteoclast. The number of TRAP-positive osteoclast was significantly reduced in cultures from either MM patients (Fig. 2A, right) or normal individuals (data not shown) exposed to IL-27 on day 3 ($P = 0.0004$) or 7 ($P = 0.003$) compared with those unexposed to the cytokine. Cultures done by adding or not hrIL-27 on day 14 and 21 (Fig. 2A, right and data not shown, respectively) contained similar proportions of osteoclast, indicating that IL-27 had to be present in the first week of culture to inhibit osteoclast differentiation.

In another set of experiments, PB $CD14^+$ monocytes from MM patients or normal donors cultured for 28 days with RANKL and M-CSF with or without hrIL-27 were subjected to the Pit assay, which measures resorbed bone area (Fig. 2B). An inhibitory effect of hrIL-27 on osteoclast activity was shown for cultures from MM patients (mean ± SD number of pits IL-27 versus control: 15,680 ± 8,700 versus 26,000 ± 7,560; $P = 0.028$; Fig. 2B). Similar results were obtained with cultures from healthy donors (data not shown).

To test the potential effect of hrIL-27 on osteoblast differentiation and function, we next analyzed WSX-1 expression on osteoblast progenitors and mature osteoblast. WSX-1 was expressed by the mature osteoblast cells Hobit (Fig. 2C, left) but not by bone marrow stromal cells (BMSC) or osteoblast progenitors (35), by flow cytometry. As shown in Fig. 2C (right), hrIL-27 significantly stimulated ($P = 0.044$) Hobit cell proliferation, whereas it did not affect (*a*) expression of the osteoblast markers Collagen I and osteocalcin (Fig. 2D, left), (*b*) expression of alkaline phosphatase, and (*c*) bone nodule formation *in vitro* (Fig. 2D, middle and right).

In additional experiments, we investigated the potential ability of BMSC to affect primary myeloma cell growth in the presence of IL-27. These experiments showed that IL-27 did not affect apoptosis of $CD138^+$ MM cells cocultured with BMSC (Fig. 2E). As expected, the presence of BMSC in coculture significantly ($P < 0.05$) reduced MM cell apoptosis (Fig. 2E).

hrIL-27 strongly inhibits tumorigenicity of NCI-H929 and U266 cells in SCID-NOD mice

The human NCI-H929, U266, JJN3, RPMI 8226, H-Sultan, OPM-2, XG-1, XG-6, and Karpas 620 MM cell lines were analyzed for gp130 and WSX-1 expression. All MM cell lines constitutively expressed the gp130 (data not shown) and the WSX-1 chains (three MM cell lines are shown in Supplementary Fig. 1). Because the NCI-H929 and the U266 cell lines show functional similarities to the primary MM cells (Supplementary Fig. 1), they were selected for *in vivo* studies. Mice injected i.p. with NCI-H929 cells and treated with hrIL-27 developed tumors significantly smaller ($P = 0.0047$) than mice inoculated with the same cells that had received PBS ($n = 16$ for both groups; hrIL27 treated: median volume, 281.6 mm^3; range, 5-784 mm^3; PBS treated: median volume, 2,882 mm^3; range, 380-6,305 mm^3; Fig. 3A, left). Similarly, mice injected s.c. with the human U266 cells and treated with hrIL-27 developed tumors significantly smaller than mice inoculated with the same cells that received PBS ($P < 0.0001$; $n = 10$ for both groups; hrIL-27 treated: median volume, 944.4 mm^3; range, 861-1,163 mm^3; PBS treated: median volume, 1,921.8 mm^3; range, 1,360-2,404 mm^3; Fig. 3A, right).

The angiogenic phenotype of tumors formed in hrIL-27 versus PBS-treated animals injected with the human MM cells was investigated. In four different experiments, two performed with tumors from animals

Published OnlineFirst June 29, 2010; DOI:10.1158/1078-0432.CCR-10-0173

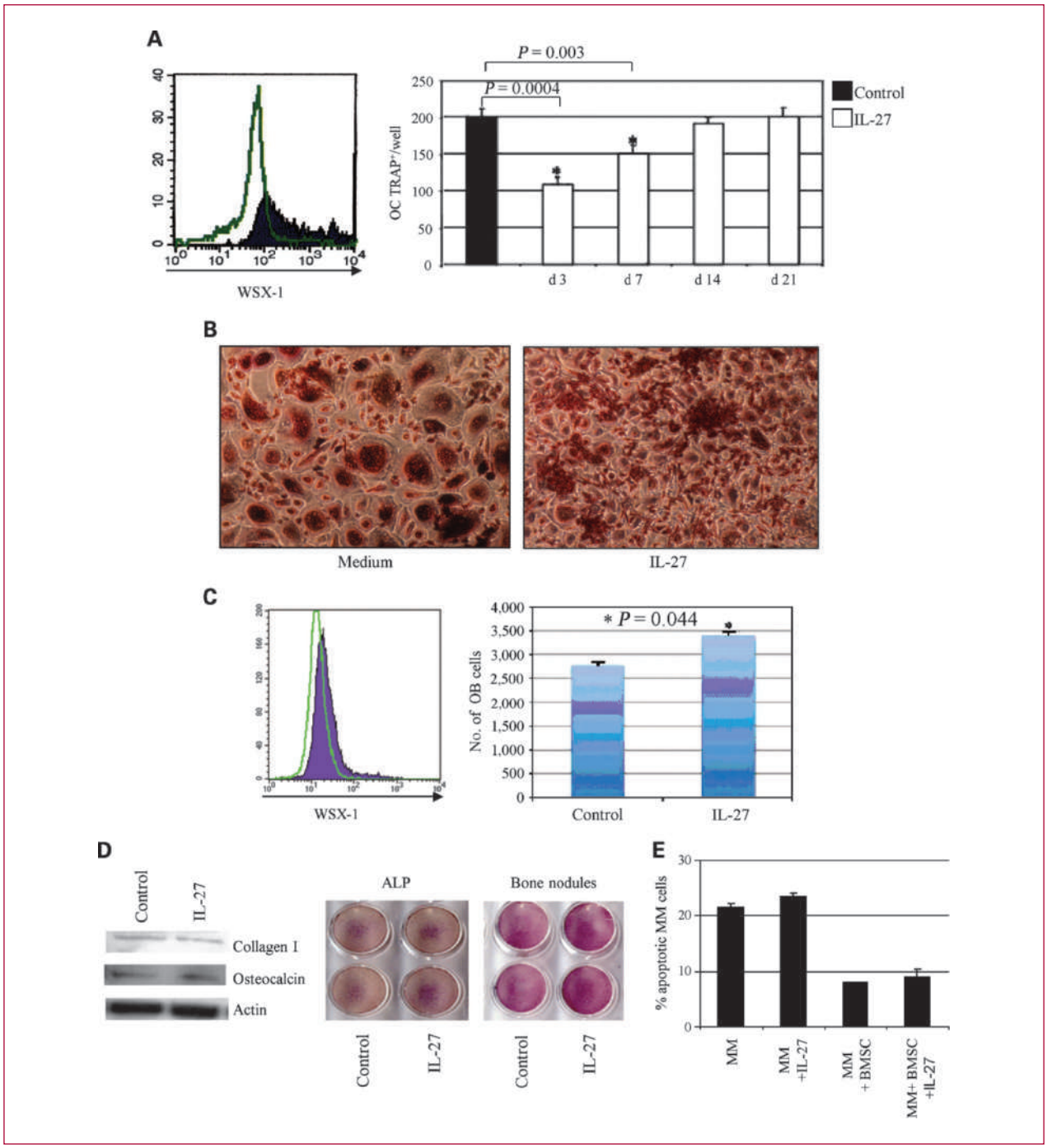

Fig. 2. A, left, WSX-1 surface expression in human CD14$^+$ cells from a MM patient. Dark profile, WSX-1 staining; open profile, isotype-matched mAb staining. Right, osteoclast generated from mononuclear cells of MM patients (n = 3) were identified as TRAP$^+$ multinucleated cells. Columns, mean number of TRAP$^+$ counted per well; bars, SD. B, pit assay was assessed using osteoclast samples generated from MM patients without (medium, left) or with (right) hrIL-27. Images shown are representative of one experiment of the three performed and were obtained on a Nikon Eclipse TE 300 microscope at 10X/0.13 using a DS-U1 digital slight and at 4×/0.12 objective lens (original magnification, ×400). C, left, WSX-1 surface expression in human osteoblastic Hobit cells. Dark profile, WSX-1 staining; open profile, isotype-matched mAb staining. Right, confluent Hobit cells were cultured with or without hrIL-27, and cell proliferation was evaluated by MTT proliferation assay. Columns, mean of cells from 10 replicate wells done in duplicate. D, left, Collagen I and osteocalcin expression in Hobit cells treated with or without hrIL-27. Actin was tested as internal control. Middle and right, alkaline phosphatase expression (middle) and bone nodule formation (right) were evaluated in Hobit cells treated with or without hrIL-27. E, apoptosis of primary MM cells cocultured with BMSC in the presence or absence of IL-27. Pooled results from two different experiments are shown. MM cells were analyzed by gating CD138$^+$ cells. MM, primary MM cells cultured with medium alone; MM+IL-27, primary MM cells cultured in the presence of IL-27; MM+BMSC, primary MM cells cocultured with medium alone in the presence of BMSC; MM+BMSC+IL-27, primary MM cells cocultured with BMSC in the presence of IL-27.

Published OnlineFirst June 29, 2010; DOI:10.1158/1078-0432.CCR-10-0173

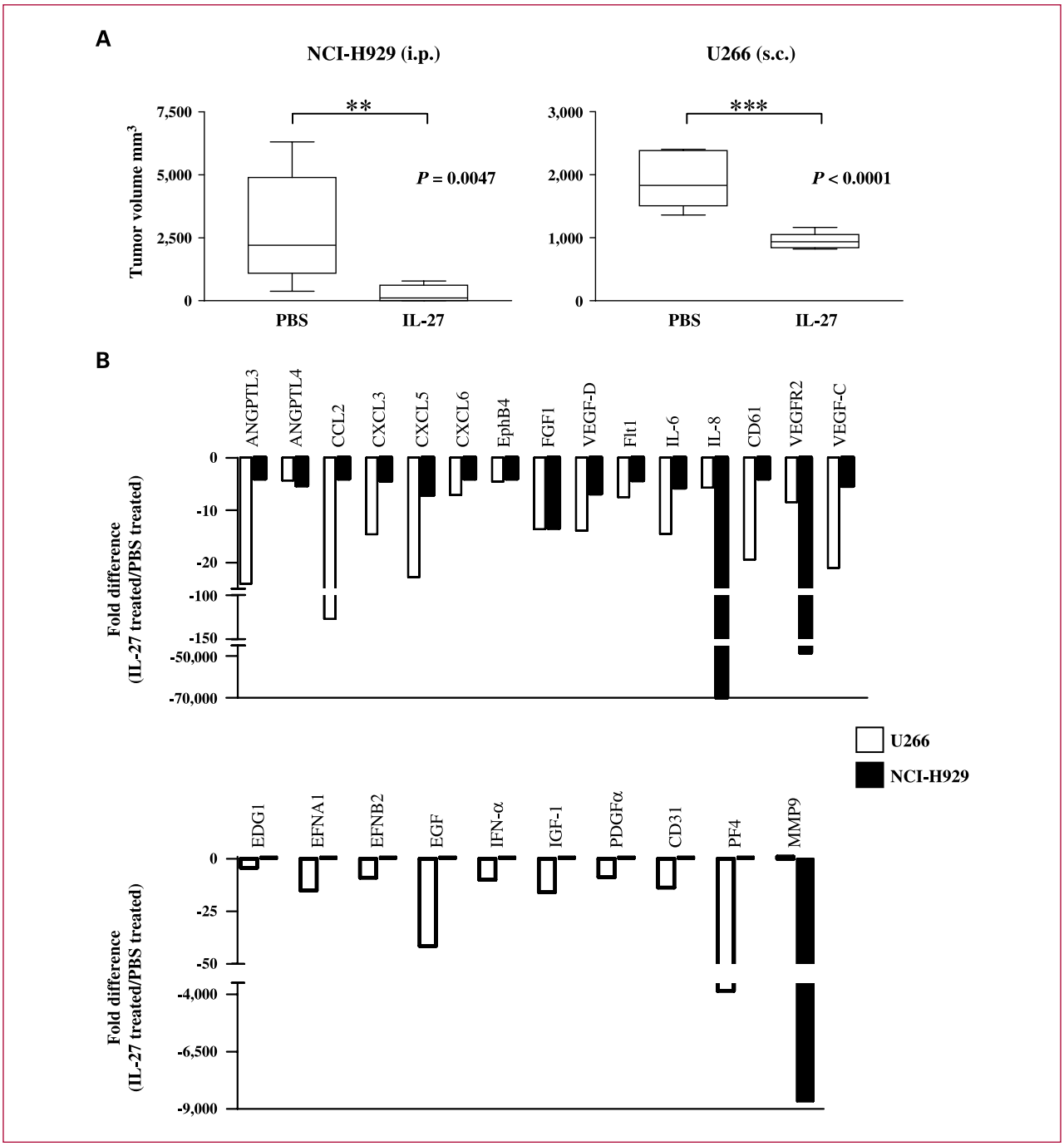

Fig. 3. A, volume of tumors grown i.p (NCI-H929 cells, PBS treated $n = 16$; hrIL-27 treated $n = 16$) and s.c. (U266 cells, PBS treated $n = 10$; hrIL-27 treated $n = 10$) in PBS- and hrIL-27-treated mice. Boxes, values between the 25th and 75th percentiles; whisker lines, highest and lowest values for each group. Horizontal lines, median values. B, tumor masses from hrIL-27– or PBS-treated mice were tested for expression of 84 human angiogenesis–related genes by PCR Array. Histogram represents fold differences of individual mRNA expression between hrIL-27 and PBS-treated mice. Top histogram, genes similarly regulated in both models; bottom histogram, genes differently regulated in both models.

injected with NCI-H929 cells and two with tumors from mice inoculated with U266 cells, the expression of a common set of proangiogenic genes was significantly ($P < 0.001$) downregulated by IL-27 treatment (ANGPTL3, ANGPTL4, CCL2, CXCL3, CXCL5, CXCL6, EphB4, FGF1, VEGF-C and VEGF-D, VEGFR2, Flt1, IL-6, IL-8, and CD61; Fig. 3B, top). Other genes were differentially regulated in the two *in vivo* models. Thus,

Published OnlineFirst June 29, 2010; DOI:10.1158/1078-0432.CCR-10-0173

MMP9 expression was downregulated only in NCI-H929 tumors formed in IL-27 versus PBS-treated mice. By contrast, expression of endoglin, ephrin A1, ephrin B2, epidermal growth factor, IFN-α, insulin-like growth factor I, platelet-derived growth factor-α, CD31, and plateled factor 4 was downregulated only in tumors formed by U266 cells in hrIL-27 versus PBS-treated animals (Fig. 3B, bottom).

Histologic and immunohistochemical features of tumors formed by NCI-H929 and U266 cells in SCID-NOD mice

PBS-treated mice, inoculated s.c. with the human U266 cells, developed poorly differentiated plasma cell myelomas, rarely showing small necrotic areas, and formed by nests of atypical cells, with occasional double nuclei and atypical mitotic figures (Fig. 4, a). These tumors were supplied by well-developed and robust vascular branches (Fig. 4, b) and showed a distinct expression of IL-6 (Fig. 4, c) and VEGF-C (Fig. 4, d). Unlike myelomas developed in control mice, those in hrIL-27–treated mice steadily showed frequent and wide ischemic-hemorrhagic necrosis (Fig. 4, e) associated with fragile and heavily damaged vascular branches (Fig. 4, f), and faint IL-6 (Fig. 4, g) and VEGF-C (Fig. 4, h) expression. No significant differences between hrIL-27–treated and control mice were observed in terms of MM cell apoptosis, proliferation, or number of murine vessels (data not shown). Tumor infiltration with host mononuclear or polymorphonuclear cells was undetectable in hrIL-27– and PBS-treated animals (data not shown). Similar histologic and immunohistochemical features were observed in tumors formed after NCI-H929 inoculation i.p. into SCID-NOD mice (data not shown).

Discussion

MM is one of the most common hematological malignancies that originates from the aberrant transformation and expansion of normal plasmablasts/plasmacells in the BM (28). MM is characterized by a strong interaction with BM microenvironment that supports tumor cell growth and spreading, and by aggressive bone destruction (28, 29).

We asked whether IL-27 may function as an antitumor agent in MM disease. Here, we showed that human primary MM cells expressed functional IL-27R, and IL-27 triggering affected their angiogenic activity, whereas it did not attract tumor cells in chemotaxis assays nor affected their apoptosis, proliferation, or cytokine release. IL-27 influenced the expression of a wide panel of angiogenesis-related genes and inhibited different proangiogenic factors such as VEGF-D and CCL2, two of the major MM growth factors (40, 41).

IL-27 has been shown to inhibit mouse osteoclast activity by acting on T lymphocytes (6), which are known to promote osteoclastogenesis in MM (37). In humans, IL-27 has been recently shown to inhibit directly *in vitro* osteoclast differentiation from mononuclear cells of normal

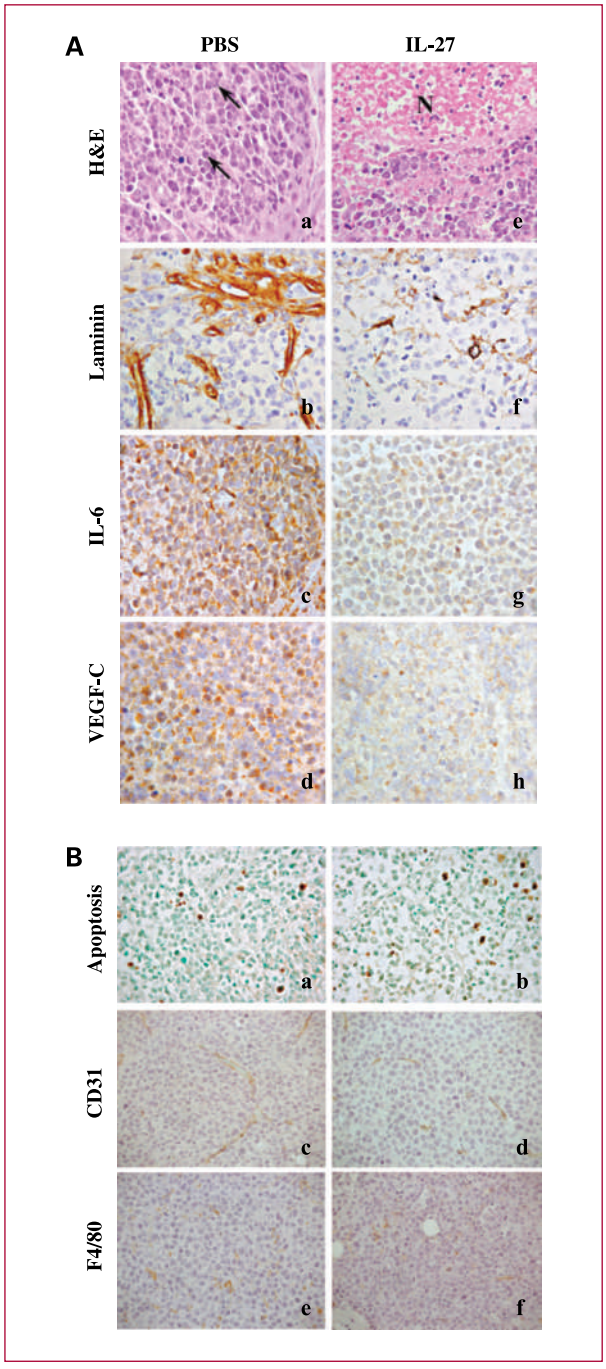

Fig. 4. A, PBS-treated mice developed a poorly differentiated plasma cell myeloma (a) formed by nests of atypical cells frequently showing atypical mitotic figures (arrows). This morphologic feature was associated with a robust vasculature, as evidenced by laminin immunostaining (b), and a distinct expression of IL-6 (c) and VEGF-C (d). By contrast, plasma cell myeloma growing in hrIL-27–treated mice (e) showed wide ischemic-hemorrhagic necrosis (N) associated with fragile and heavily damaged vascular branches (f) and a very weak IL-6 (g) and VEGF-C (h) expression. B, terminal deoxynucleotidyl transferase–mediated dUTP nick end labeling assay (apoptosis), murine vessel (CD31), and macrophage infiltration (F4/80) in tumors from PBS-treated (a, c, and e) and hrIL-27-treated (b, d, and f) animals injected with the human U266 cell line.

Published OnlineFirst June 29, 2010; DOI:10.1158/1078-0432.CCR-10-0173

individuals (42). Whether or not IL-27 can exert a similar activity in MM patients was unknown. Here, we showed that osteoclast progenitors from MM patients and controls expressed functional IL-27R, and that IL-27 directly dampened osteoclast differentiation and bone lytic activity. IL-27–driven inhibition of the latter activity is consistent with impairment of osteoclast differentiation operated by the cytokine.

The balance between osteoclast and osteoblast activity plays a key role in bone remodeling because it reflects the balance between bone destruction and new bone formation (43). In advanced metastatic MM, the aberrant proliferation and activation of osteoclasts overcomes osteoblast activity so strongly that apoptotic osteoblasts can be observed in lesion sites (44). In this context, we showed that IL-27 induced proliferation in Hobit cells representing an immortalized mature osteoblast cell line. However, IL-27 did not affect other osteoblast activities such as expression of the osteoblast markers Collagen I and osteocalcin, expression of alkaline phosphatase, and bone nodule formation. Thus, IL-27 seems to amplify the mature osteoblastic compartment without affecting its functionality. Other molecules present in the bone microenvironment would complement IL-27 activity by modulating osteoblast function (40).

In immunodeficient SCID-NOD mice injected with two different MM cell lines using two different routes of inoculation, hrIL-27 strongly inhibited tumor growth. The key mechanism involved in such effect was the inhibition of angiogenesis, which caused ischemic necrosis in the tumors. IL-27 induced the downregulation of different proangiogenic molecules, including some MM growth factors, such as IL-6, VEGF-D, and CCL2 (40, 41). Although VEGF-D and CCL2 were downregulated in tumors formed in IL-27–treated mice and in IL-27 *in vitro* treated primary MM cells, IL-6 was not detected in primary MM cells. The latter finding is consistent with previous demonstration (45) that IL-6 is a paracrine growth factor produced by stromal cells in BM microenvironment and not by MM cells themselves.

The use of SCID-NOD mice allowed us to evaluate the antitumor activity of human IL-27 on human MM cells *in vivo* in the absence of immune responses. Although human IL-27 is not specie specific (2), the following findings support the conclusion that, in our model, the cytokine targeted directly human MM cells: (*a*) the *in vivo* antitumor mechanisms operated by IL-27 overlapped with those observed *in vitro* in MM cells, and (*b*) tumor infiltration with host mononuclear or polymorphonuclear cells was virtually undetectable. Moreover, tumors formed in IL-27 versus PBS-treated SCID-NOD mice injected with MM cell lines showed no differences in terms of number of murine vessels. The latter finding indicated that IL-27–mediated inhibition of angiogenesis was completely dependent on the direct effect of the cytokine on human MM cells that damped the formation of tumor-derived endothelial microvessels (46–48).

Taken together, our findings showed for the first time that human IL-27 acts as a potent antitumor agent for MM that may block MM progression and metastatic bone resorption. Additional antitumor effects may be operated *in vivo* by IL-27 through enhancement of CTL, natural killer, and $CD8^+$ T-cell cytotoxicity (1). On this ground, IL-27 seems to represent a novel, promising therapeutic agent for MM patients, whose prognosis remains grim, based on its multifunctional activity. An additional argument in favor of this proposal is the low toxicity shown by IL-27 in animal models, likely in relation to the low induction of IFN-γ *in vivo* (21).

Disclosure of Potential Conflicts of Interest

No potential conflicts of interest were disclosed.

Grant Support

Grants from Associazione Italiana per la Ricerca sul Cancro, Milano, Italy grant no. 4014 (I. Airoldi) and Fondazione Cassa di Risparmio della Provincia di Chieti (CariChieti), Italy (E.D. Carlo)

The costs of publication of this article were defrayed in part by the payment of page charges. This article must therefore be hereby marked *advertisement* in accordance with 18 U.S.C. Section 1734 solely to indicate this fact.

Received 01/20/2010; revised 04/19/2010; accepted 06/08/2010; published OnlineFirst 06/29/2010.

References

1. Trinchieri G, Pflanz S, Kastelein RA. The IL-12 family of heterodimeric cytokines: new players in the regulation of T cell responses. Immunity 2003;19:641–4.
2. Pflanz S, Timans JC, Cheung J, et al. IL-27, a heterodimeric cytokine composed of EBI3 and p28 protein, induces proliferation of naive CD4(+) T cells. Immunity 2002;16:779–90.
3. Artis D, Villarino A, Silverman M, et al. The IL-27 receptor (WSX-1) is an inhibitor of innate and adaptive elements of type 2 immunity. J Immunol 2004;173:5626–34.
4. Feng XM, Chen XL, Liu N, et al. Interleukin-27 upregulates major histocompatibility complex class II expression in primary human endothelial cells through induction of major histocompatibility complex class II transactivator. Hum Immunol 2007;68:965–72.
5. Villarino AV, Larkin J III, Saris CJ, et al. Positive and negative regulation of the IL-27 receptor during lymphoid cell activation. J Immunol 2005;174:7684–91.
6. Kamiya S, Nakamura C, Fukawa T, et al. Effects of IL-23 and IL-27 on osteoblasts and osteoclasts: inhibitory effects on osteoclast differentiation. J Bone Miner Metab 2007;25:277–85.
7. Larousserie F, Charlot P, Bardel E, Froger J, Kastelein RA, Devergne O. Differential effects of IL-27 on human B cell subsets. J Immunol 2006; 176:5890–7.
8. Chen Q, Ghilardi N, Wang H, et al. Development of Th1-type immune responses requires the type I cytokine receptor TCCR. Nature 2000; 407:916–20.
9. Pflanz S, Hibbert L, Mattson J, et al. WSX-1 and glycoprotein 130 constitute a signal-transducing receptor for IL-27. J Immunol 2004;172: 2225–31.

Published OnlineFirst June 29, 2010; DOI:10.1158/1078-0432.CCR-10-0173

10. Villarino AV, Huang E, Hunter CA. Understanding the pro- and anti-inflammatory properties of IL-27. J Immunol 2004;173:715–20.
11. Villarino AV, Hunter CA. Biology of recently discovered cytokines: discerning the pro- and anti-inflammatory properties of interleukin-27. Arthritis Res Ther 2004;6:225–33.
12. Hamano S, Himeno K, Miyazaki Y, et al. WSX-1 is required for resistance to Trypanosoma cruzi infection by regulation of proinflammatory cytokine production. Immunity 2003;19:657–67.
13. Pearl JE, Khader SA, Solache A, et al. IL-27 signaling compromises control of bacterial growth in mycobacteria-infected mice. J Immunol 2004;173:7490–6.
14. Yamanaka A, Hamano S, Miyazaki Y, et al. Hyperproduction of proinflammatory cytokines by WSX-1-deficient NKT cells in concanavalin A-induced hepatitis. J Immunol 2004;172:3590–6.
15. Batten M, Li J, Yi S, et al. Interleukin 27 limits autoimmune encephalomyelitis by suppressing the development of interleukin 17-producing T cells. Nat Immunol 2006;7:929–36.
16. Stumhofer JS, Laurence A, Wilson EH, et al. Interleukin 27 negatively regulates the development of interleukin 17-producing T helper cells during chronic inflammation of the central nervous system. Nat Immunol 2006;7:937–45.
17. Miyazaki Y, Inoue H, Matsumura M, et al. Exacerbation of experimental allergic asthma by augmented Th2 responses in WSX-1-deficient mice. J Immunol 2005;175:2401–7.
18. Shimizu S, Sugiyama N, Masutani K, et al. Membranous glomerulonephritis development with Th2-type immune deviations in MRL/lpr mice deficient for IL-27 receptor (WSX-1). J Immunol 2005;175:7185–92.
19. Neufert C, Becker C, Wirtz S, et al. IL-27 controls the development of inducible regulatory T cells and Th17 cells via differential effects on STAT1. Eur J Immunol 2007;37:1809–16.
20. Hisada M, Kamiya S, Fujita K, et al. Potent antitumor activity of interleukin-27. Cancer Res 2004;64:1152–6.
21. Oniki S, Nagai H, Horikawa T, et al. Interleukin-23 and interleukin-27 exert quite different antitumor and vaccine effects on poorly immunogenic melanoma. Cancer Res 2006;66:6395–404.
22. Shimizu M, Shimamura M, Owaki T, et al. Antiangiogenic and antitumor activities of IL-27. J Immunol 2006;176:7317–24.
23. Airoldi I, Di Carlo E, Banelli B, et al. The IL-12Rβ2 gene functions as a tumor suppressor in human B cell malignancies. J Clin Invest 2004;113:1651–9.
24. Airoldi I, Di Carlo E, Cocco C, et al. IL-12 can target human lung adenocarcinoma cells and normal bronchial epithelial cells surrounding tumor lesions. PLoS One 2009;4:e6119.
25. Airoldi I, Di Carlo E, Cocco C, et al. Endogenous IL-12 triggers an antiangiogenic program in melanoma cells. Proc Natl Acad Sci U S A 2007;104:3996–4001.
26. Airoldi I, Cocco C, Giuliani N, et al. Constitutive expression of IL-12R β 2 on human multiple myeloma cells delineates a novel therapeutic target. Blood 2008;112:750–9.
27. Yoshimoto T, Morishima N, Mizoguchi I, et al. Antiproliferative activity of IL-27 on melanoma. J Immunol 2008;180:6527–35.
28. Kyle RA, Rajkumar SV. Multiple myeloma. N Engl J Med 2004;351:1860–73.
29. Roodman GD. Role of the bone marrow microenvironment in multiple myeloma. J Bone Miner Res 2002;17:1921–5.
30. Ribatti D, Nico B, Vacca A. Importance of the bone marrow microenvironment in inducing the angiogenic response in multiple myeloma. Oncogene 2006;25:4257–66.
31. Vacca A, Ribatti D. Bone marrow angiogenesis in multiple myeloma. Leukemia 2006;20:193–9.
32. Strobeck M. Multiple myeloma therapies. Nat Rev Drug Discov 2007;6:181–2.
33. Durie BG, Salmon SE. A clinical staging system for multiple myeloma. Correlation of measured myeloma cell mass with presenting clinical features, response to treatment, and survival. Cancer 1975;36:842–54.
34. Keeting PE, Rifas L, Harris SA, et al. Evidence for interleukin-1 β production by cultured normal human osteoblast-like cells. J Bone Miner Res 1991;6:827–33.
35. Giuliani N, Colla S, Morandi F, et al. Myeloma cells block RUNX2/CBFA1 activity in human bone marrow osteoblast progenitors and inhibit osteoblast formation and differentiation. Blood 2005;106:2472–83.
36. Ribatti D, Gualandris A, Bastaki M, et al. New model for the study of angiogenesis and antiangiogenesis in the chick embryo chorioallantoic membrane: the gelatin sponge/chorioallantoic membrane assay. J Vasc Res 1997;34:455–63.
37. Giuliani N, Colla S, Sala R, et al. Human myeloma cells stimulate the receptor activator of nuclear factor-κ B ligand (RANKL) in T lymphocytes: a potential role in multiple myeloma bone disease. Blood 2002;100:4615–21.
38. Schmittgen LivakKJ. Analysis of relative gene expression data using real-time quantitative PCR and the 2(-Δ Δ C(T)) Method. Methods 2001;25:402–8.
39. Vacca A, Ribatti D, Presta M, et al. Bone marrow neovascularization, plasma cell angiogenic potential, and matrix metalloproteinase-2 secretion parallel progression of human multiple myeloma. Blood 1999;93:3064–73.
40. Aggarwal R, Ghobrial IM, Roodman GD. Chemokines in multiple myeloma. Exp Hematol 2006;34:1289–95.
41. Ria R, Roccaro AM, Merchionne F, Vacca A, Dammacco F, Ribatti D. Vascular endothelial growth factor and its receptors in multiple myeloma. Leukemia 2003;17:1961–6.
42. Furukawa M, Takaishi H, Takito J, et al. IL-27 abrogates receptor activator of NF-κ B ligand-mediated osteoclastogenesis of human granulocyte-macrophage colony-forming unit cells through STAT1-dependent inhibition of c-Fos. J Immunol 2009;183:2397–406.
43. Bataille R, Chappard D, Marcelli C, et al. Mechanisms of bone destruction in multiple myeloma: the importance of an unbalanced process in determining the severity of lytic bone disease. J Clin Oncol 1989;7:1909–14.
44. Taube T, Beneton MN, McCloskey EV, Rogers S, Greaves M, Kanis JA. Abnormal bone remodelling in patients with myelomatosis and normal biochemical indices of bone resorption. Eur J Haematol 1992;49:192–8.
45. Gunn WG, Conley A, Deininger L, Olson SD, Prockop DJ, Gregory CA. A crosstalk between myeloma cells and marrow stromal cells stimulates production of DKK1 and interleukin-6: a potential role in the development of lytic bone disease and tumor progression in multiple myeloma. Stem Cells 2006;24:986–91.
46. Maniotis AJ, Folberg R, Hess A, et al. Vascular channel formation by human melanoma cells *in vivo* and *in vitro*: vasculogenic mimicry. Am J Pathol 1999;155:739–52.
47. Pezzolo A, Parodi F, Corrias MV, Cinti R, Gambini C, Pistoia V. Tumor origin of endothelial cells in human neuroblastoma. J Clin Oncol 2007;25:376–83.
48. Streubel B, Chott A, Huber D, et al. Lymphoma-specific genetic aberrations in microvascular endothelial cells in B-cell lymphomas. N Engl J Med 2004;351:250–9.